Experiences with a Ku-Band Microwave Fourier Transform Spectrometer

G. Bestmann, H. Dreizler, H. Mäder, and U. Andresen
Abteilung Chemische Physik im Institut für Physikalische Chemie der Universität Kiel

Z. Naturforsch. **35a**, 392–402 (1980); received February 12, 1980

The construction of a Ku-band microwave Fourier transform spectrometer is described in detail. The optimal cell length, sensitivity and resolution is discussed. Some sample spectra of SO_2 and OCS isotopes are given.

It is well known that Fourier transform (FT) spectroscopy in the near and far infrared [1, 2] has several advantages in comparison to conventional methods. The same may be stated for Fourier transform NMR spectroscopy [3]. Recently the FT-technique was extended to the microwave region [4]. Ekkers and Flygare [5] reported a construction for the band of 4 to 8 GHz.

We decided to construct a MW-FT-spectrometer in the region of 12 to 18 GHz, which seems presently the highest frequency region for such a type of spectrometer, as certain microwave parts are not yet commercially available for higher frequencies. We present in detail our construction, a discussion of optimal cell length, sensitivity and resolution and our experiences. Some results have been published recently [6, 7].

Apparatus

A block diagram of the spectrometer is shown in Figure 1. Details are given in Figs. 2 to 8.

The signal source (2) is a phase stabilized backward wave oscillator (BWO). The CW-microwave is pulse modulated and amplified with a travelling wave tube amplifier (TWT) (3). In the sample cell (4) the ensemble of molecules is polarized [8]. The transient emission signal of the molecules is superheterodyne detected in (5 a) and converted to a 0 to 50 MHz IF signal with a phase stabilized CW-MW local frequency (6) and a 130 MHz RF-frequency (5 b). With a 1 bit transient recorder/digital averager (7 a) the IF signal is digitized and averaged if the signal power to noise power ratio S/N is less than 1/2.

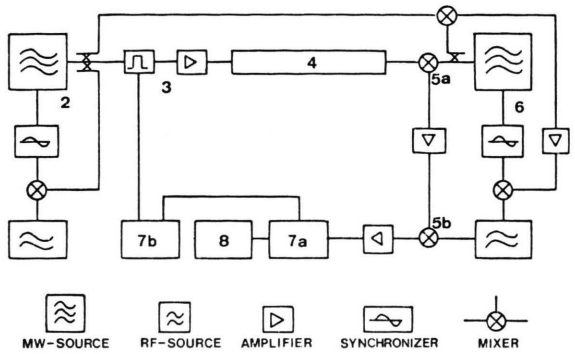

Fig. 1. Blockdiagram Ku-Band MW-FT spectrometer. 2 Phase stabilized MW signal source; 3 Pulse generation and amplification; 4 Sample cell; 5a MW mixer; 5b IF mixer; 6 Phase stabilized MW local source; 7a 1-bit transient recorder/digital averager; 8 Computer; 7b Controller.

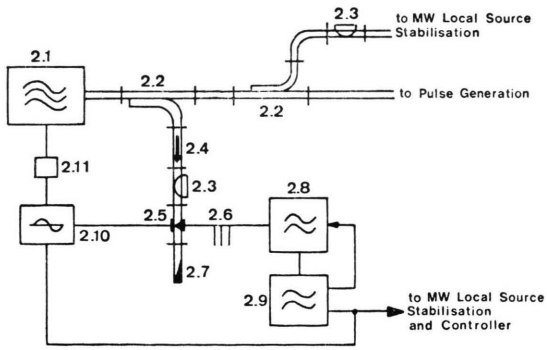

Fig. 2. Phase stabilized MW signal source and frequency reference. 2.1 MW-Sweeper Hewlett-Packard 8690 B with a 8695 A BWO-drawer; 2.2 Directional coupler, 10 dB; 2.3 Variable attenuator, 0 to 30 dB; 2.4 Waveguide isolator, 30 dB isolation; 2.5 Waveguide mixer with 1N78 or 1N26; 2.6 Triple-stub tuner; 2.7 Termination; 2.8 Normal frequency generator, Rohde & Schwarz XUC; 2.9 Synthesizer, Rohde & Schwarz SMDH. The quartz oscillator is the frequency-reference of the spectrometer. 2.10 Synchronizer, Schomandl FDS 30 or Rohde & Schwarz XUC or Hewlett-Packard 8709A with a 20 MHz converter for reference. 2.11 RC filter.

Reprint request to Prof. Dr. H. Dreizler, Abt. Chemische Physik im Institut für Physikalische Chemie der Universität Kiel, Olshausenstr. 40/60 D-2300 Kiel.

0340-4811 / 80 / 0400-0392 $ 01.00/0. — Please order a reprint rather than making your own copy.

For transient signals with $S/N > \frac{1}{2}$ a Biomation 6500 waveform recorder together with a Fabri-Tek 1072 averager is used. The computer (8) prepares the data, if necessary by additional averaging and calculates the spectrum by a Fourier transformation or evaluates the relaxation time. The controller (7 b) synchronizes the pulse generation and the signal conversion.

The frequencies are referred to a quartz oscillator * of high precision which is regularily compared to the normal frequency of 77.5 kHz of the DCF 77 Mainflingen radio station/Germany.

In Fig. 2 we give the details of the phase stabilized CW signal source. The main problem is to produce a MW signal of known frequency and high spectral purity which is especially free of modulations, as those may be a source of coherent disturbances **.

So the mixer (2.5) is arranged in the side arm isolated by the attenuator (2.3) and isolator (2.4). Further oscillations in the phase lock loop should be minimized. This is done by a proper setting of the synchronizer (2.10) and the RC filter (2.11). It is also important to prevent a leakage of the MW out off the waveguide and cable connectors.

The MW pulse generation and amplification is presented in Figure 3. The MW pulses are generated with the switches (3.4) and (3.5). The minimum length of a pulse with full amplitude is 10 ns as the rise and fall times of the switches are in the order of 5 ns. The isolator (3.3) and attenuator (3.1) prevents a disturbance of the MW source by reflected MW power when the switches are closed. The switches are opened in overlapping time intervals to produce pulses of variable length (compare Figure 8). We have selected this switch type as rise time (5 ns), isolation (80 dB), insertion loss (specified max. 3 dB, measured 2 dB) and power compatibility is excellent. The low power MW pulses are fed to the TWT amplifier (3.6) by a low VSWR coaxial to waveguide transition (3.7). The amplitude of the pulses is controlled by the attenuator (3.1). The amplified MW pulses reach the sample cell (4) by an isolator (3.8) and the switch (3.9). The isolator (3.8) protects the TWT against reflected MW power. Switch (3.9), which is open for the MW pulse, cuts off TWT noise from the detection system (5) during the measuring period by 80 dB. The optocoupler and driver unit (3.10) rejects reflected command pulses on the long cables from the controller (7 b) and avoids ground loops. A sufficient shielding is also necessary in this part of the spectrometer. All connections on the MW pulse path are made as short as possible to reduce the time of disturbance by reflected pulses.

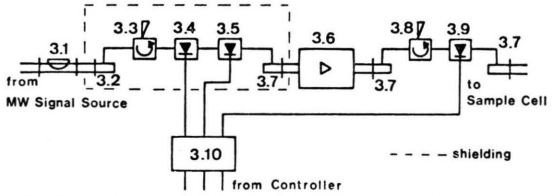

Fig. 3. Pulse generation and amplification. 3.1 Attenuator; 3.2 Waveguide to coax transition; 3.3, 3.8 Coaxial isolator, 18 dB isolation; 3.4, 3.5 and 3.9 Pin-diode-switch, Hewlett Packard 33144 A with driver 33190 A; 3.6 TWT-Amplifier, Hughes 1177 A (10 W); 3.7 Low VSWR (< 1.10) waveguide to coax transition; 3.10 Line-receiver and driver (optocoupler), power supply.

* Presently the A/D-conversion step width is referred to a separate 100 MHz quartz. It will be replaced by a synchronized oscillator.

** We avoid the term "coherent noise" as noise is a statistical phenomenon.

Some features of the sample cell (4) have to be considered in connection with Figure 4. For an optimum performance of the spectrometer the molecules in the cell (4.3) should be polarized by an incident MW pulse of suitable length (near $\pi/2$-pulse) only once. This pulse must be prevented from reaching the detection system (4) which is made by a proper timing of the closing period of the switch (4.5) (comp. Figure 8). As the closed switch (4.5) reflects the incident power a pulse travels back to the sample cell. A multiple polarization and an interference with the transient signal in the detection system (5) is minimized and shortened by insertion of four low VSWR waveguide isolators (4.2) and (4.4). So the sample cell of 12 m length is divided into three sections of 4 m length each. By the use of four isolators the reflected pulse which again reaches the cell end after approximately 80 ns is attenuated at least by 120 dB in comparison to 30 dB, if only isolator (4.4) is used. The polarizing pulse at the cell end is typically between 15 and 26 dBm. So the reflected pulse compares to a transient signal, which was measured for $OC^{34}S$ ($\alpha = 3 \cdot 10^{-7}\,cm^{-1}$) as typically -76 dBm. (Estimated from theory for plane waves -80 dBm). By this arrangement the measurement of the transient signal may be started earlier.

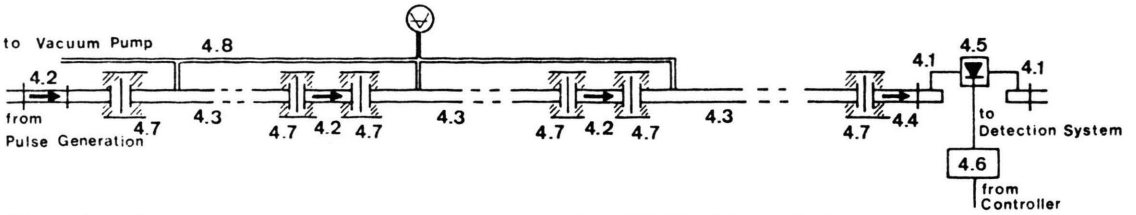

Fig. 4. Sample cell. 4.1 Waveguide to coax transition, low VSWR; 4.2, 4.4 Isolator, low input and output VSWR (<1.10) isolation 30 dB, insertion loss <1 dB; 4.3 Sample cell section, 4 m length, Ku-band; 4.5 PIN diode switch, see Fig. 3; 4.6 Power supply; 4.7 Shielded MW windows; 4.8 Vacuum system with MKS-Baratron 170 M — 6B vacuum meter.

We tested also a SPDT switch (General Microwave F 8928) with a termination on one end. The performance was not better.

The cell windows were found to leake MW power. We shielded the windows by copper tubes and MW absorbing material. Presently the isolators (4.2) between the three segments of the sample cell (4.3) are enclosed by windows. We intend to avoid these reflection points by a special construction. The connection of the vacuum system (4.8) to the sample cell is made by small holes of 1 mm diameter to minimize reflections. This leads to a large evacuation time. In order to decrease this time a special connection was built, where a piece of waveguide is removed during the evacuation period and is inserted during measurements. The cell may be cooled to $-65\,^{\circ}C$ with liquid methanol (cryomat Lauda K90SW) flowing through a cooling jacket.

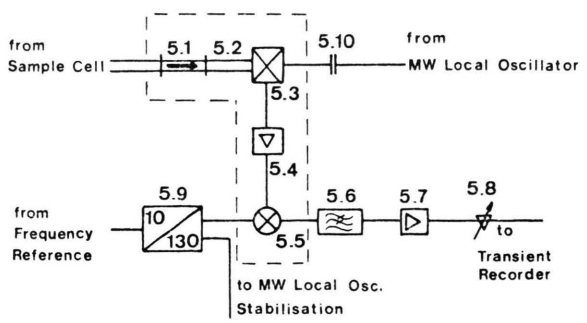

Fig. 5. Detection system. 5.1 Isolator, see 4.2 and 4.4; 5.2 High-pass-filter, Ku-band waveguide; 5.3 Orthoguide mixer with integrated preamplifier RHG WMP 12—18 BG54, local power + 8 dBm, IF bandwidth 65 MHz, IF gain 22.5 dB, noise figure (NF) 7.3 dB; 5.4 Amplifier RHG ICFV 16060, IF bandwidth 60 MHz gain 20 dB, NF 3 dB; 5.5 IF-mixer, Mini Circuits ZAD-1, 0.5—500 MHz, conversion loss 6 dB; 5.6 Low pass filter 50 MHz, 5 sections; 5.7 Amplifier, Avantec GPD 462 and 463, gain 29 dB, NF 5 dB; 5.8 Variable attenuator; 5.9 Frequency multiplier 10 to 130 MHz, harmonic suppression >80 dB for harmonics of 10 MHz; 5.10 DC-Block, inner- outer.

In Fig. 5 the MW and IF mixer is shown. An isolator (5.1) reduces reflections. The waveguide (5.2) acts as a high pass filter to suppress harmonics of the PIN switch (4.5). A residual switch transient still prevents from starting the measurements earlier than 300 ns after the end of the polarizing pulse. In the mixer the transient MW signal is mixed with the MW of the local oscillator (6). The IF signal with a center frequency of 160 MHz is amplified by (5.4) and converted to a signal with a center frequency of 30 MHz and band-limited to 50 MHz by the low pass filter (5.6). As tested in narrow band from 11.2 to 11.8 GHz a low noise microwave amplifier * reduces the noise figure of our detection system and the influence of coherent disturbances by increasing the signal level at the mixer. The amplifier was inserted in front of the isolator (5.1). One or two units of (5.7) are used as postamplifier. It is important, that the IF local frequency is spectral pure. By using several filters and amplifiers, we obtain a 130 MHz signal which is 80 dB above other harmonics of 10 MHz.

Figure 6 shows the phase stabilization of the MW local oscillator which should be of high spectral purity. It is phase stabilized 160 MHz above or below the signal frequency by the mixer (6.3), the filter (6.5), the amplifier (6.6), the IF mixer (6.7) and the synchronizer (6.8). The second mixing is necessary as the synchronizer (6.8) works at 30 MHz. The isolators (6.2) and (6.4) reduce modulation on the MW signal and local frequency. We choose the IF of 160 MHz as commercial parts are available with a sufficient bandwidth and smooth characteristics within the bandwidth. We found no difference in performance, when using a BWO or a YIG tuned Gunn oscillator as the MW local source.

* Miteq AMF-3A-/112-1, NF 3.9 dB, gain 23 dB.

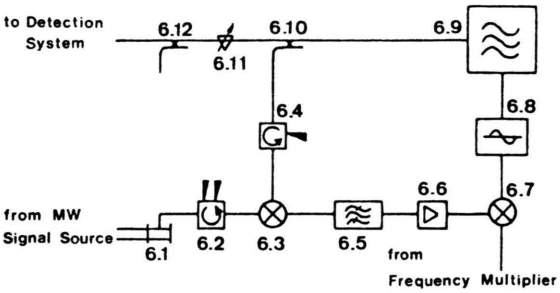

Fig. 6. MW local oscillator. 6.1 Waveguide to coax transition; 6.2 Coaxial isolator, 35 dB isolation; 6.3 MW mixer Watkins-Johnsen M17C; 6.4 Coaxial isolator, 17 dB isolation; 6.5 Band-pass-filter, 160 MHz with 10 MHz bandwidth; 6.6 Amplifier 40 dB, NF 2.5 dB; 6.7 IF mixer, Mini Circuits ZAY-3; 6.8 Synchronizer, Schomandl FDS 30; 6.9 MW local oscillator, Hewlett Packard 8690B with 8695A BWO plug in unit or YIG-tuned oscillator, Systron-Donner SDYX 3001 with power supply; 6.10 Directional coupler 20 dB; 6.11 Variable attenuator; 6.12 Directional coupler 10 dB for power meter.

A vital part of the spectrometer is the 1-bit transient recorder/digital averager (7 a). A block diagram is shown together with the controller (7 b) in Figure 7. The transient signals are given by the detection system (5) as a band-limited signal of some microseconds duration in the range from 0 to 50 MHz. For weak spectral lines the S/N ratio is smaller than 1/2.

To account for the sampling theorem [9] the transient signal has to be digitized with a rate equal to or higher than 100 MHz or a step width equal to or less than $\Delta t = 10$ ns.

To improve the S/N-ratio for a weak spectrum a large number of single measurements have to be averaged synchronously. For a S/N-ratio smaller than 1/2 our 1-bit A/D-converter * is sufficient and converts the signal almost linearly.

To exploit fully the FT method the repetition rate of the measurement following the polarization by the MW pulse has to be high. The rotational relaxation time T_2 sets an upper limit in the order of 200 kHz. With the present technology this could be reached at high cost. As a compromise we reduced the maximum repetition rate to 18 kHz ** which leads to a reduction of the obtainable S/N-ratio by a factor of three

Our instrument has presently a digitizing rate of 100 MHz [a] and takes 256, 512 or 1024 sample points of the transient signal. For one transient signal this results in a measuring time T of 2.56, 5.12 or 10.24 µs respectively, a time which limits the resolution. The averager has a word length of 16 bit [b]. The measurement of noise, which generates statistically zero or one, leads after 128 K ($K = 1024$) averaging cycles to an overflow [c]. This does not limit the

* In a 1-bit A/D conversion the signal is compared to a reference voltage.

** for 256 data points, 5 kHz for 1024 data points.

[a] A modification to 100, 50, 20 and 10 MHz is under construction.

[b] Extension to 20 or 24 bit under construction.

[c] This was tested with noise of suitable amplitude.

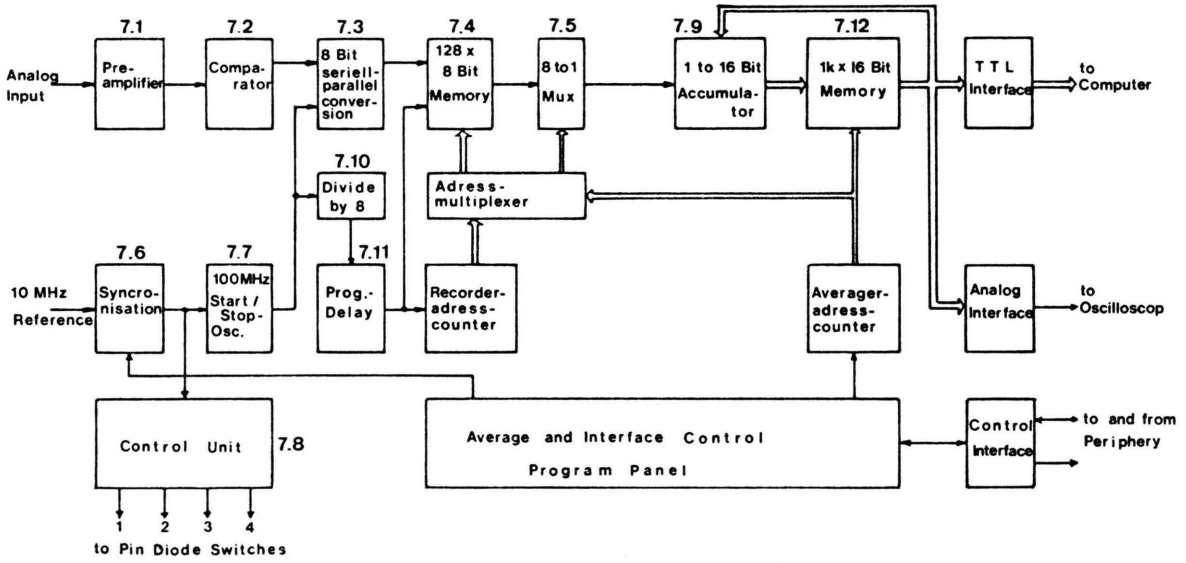

Fig. 7. Block diagram of the 1-bit transient recorder/digital averager.

number of averaging cycles, especially for weak signals, if the averaged signal is within the range of 16 bit. The construction of the transient recorder/digital averager is shown in Figure 7.

The analog input signal is preamplified by a shielded unit (7.1) and discriminated to be of positive or negative voltage (7.2). The comparator (7.2) transfers the results in series to a 8 bit shift register (7.3) with a rate of 100 MHz. Via the parallel output of (7.3) the data are transfered 8 bit in parallel to a buffer of 128×8 bit (7.4). The correct order of the data is restored during the read out by a 8 to 1 multiplexer (7.5).

To synchronize the experiment with the data acquisition the start signal is referred to the 10 MHz reference frequency of the spectrometer (7.6). The start signal triggers the controller (7.8) and a 100 MHz start-stop quartz oscillator (7.7). This oscillator provides the digitizing rate or the time interval between the data points. As the precision of the digitizing rate contributes to the accuracy of the MW frequency determination of a line we preferred a quartz rather than a free running oscillator [5]. This oscillator determines also the transfer rate from (7.3) to (7.4) and the address advance of the recorder address counter. The data acquisition may be shifted with respect to the starting point of the experiment by a programmable delay (7.11). During the data acquisition the 10 MHz reference frequency is switched off to reduce interference.

After acquisition the data are read in series from (7.9) and added to the contents of the $1\,\mathrm{K} \times 16$ bit memory (7.12) with a cycle time of 200 ns. This limits the repetition rate of the experiments to 18 kHz for 256 data points. After averaging the data may be displayed on an oscilloscope or transfered to the computer (Figures 1, no. 8).

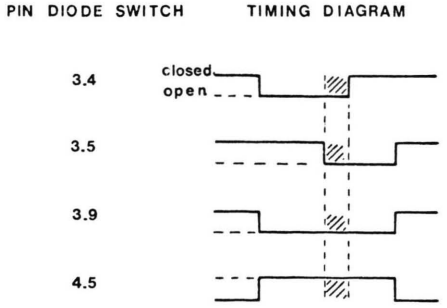

Fig. 8. Timing of the command pulses for the PIN diode switches.

For a transient signal with $S/N > 1/2$ the 1-bit transient recorder has to be replaced by the Biomation 6500 6-bit transient recorder together with a Fabri-Tek 1072 averager. The maximum digitizing rate is 500 MHz at 1024 data points. As the transfer time is limited by the Fabri-Tek to about 10 µs per point the repetition rate of measurement is only 100 Hz. This is not a severe limitation as with a better S/N ratio less averaging cycles are necessary. After averaging the data are handled in the same way as above.

The controller (7.8) provides the command pulses for the switches (3.4), (3.5), (3.9) and (4.5) according to Figure 8. By the switches (3.4) and (3.5) a MW pulse of variable length is generated by overlapping "open"-states. The pulse length may be varied from 0 to 200 ns.

The computer (Figs. 1, no. 8) is a minicomputer Texas Instruments TI 990/10 with a 64 K byte memory. A typical command time is 6 µs. The computer is used to handle the data by further averaging if necessary and by calculating the spectrum with a Cooley-Tuckey Fast Fourier transform algorithm. The transformation takes 7 s for 1024 data points. The spectrum may be displayed on a X-Y-recorder.

As an example Fig. 9 d, c gives an averaged signal and Fourier transformed spectrum.

Optimum cell length

We now proceed and discuss theoretical expressions which relate the amplitude of the emitted field at the detector to the length of the sample cell. The treatment includes the effects of the cell attenuation which has not been considered so far in the theoretical description of transient emission experiments. As result an estimate of the optimum cell length is obtained.

As shown in the appendix, the electric field amplitude E_{em} of the emitted microwave radiation for a rectangular waveguide with cross section $a \times b$ $(0 \leqq x \leqq a,\ 0 \leqq y \leqq b,\ a > b)$ and length $L (0 \leqq z \leqq L)$ is at $x = a/2$ and $z = L$ given by

$$E_{\mathrm{em}} = -\frac{\pi\,\omega\,\hbar\,\varkappa\,\Delta N_0}{c_g}\, e^{-\alpha_g L/2} \left\{ \int_0^L J_1 (\varkappa\,\varepsilon_0\,t_p\, e^{-\alpha_g z/2}) \cdot e^{\alpha_g z/2} \mathrm{d}z \right\} e^{-(t-\tau_1)/T_2}\,. \tag{1}$$

To derive (1) wave propagation in the TE_{10}-mode has been assumed and effects of the molecular velocity distribution have been neglected. ω is the

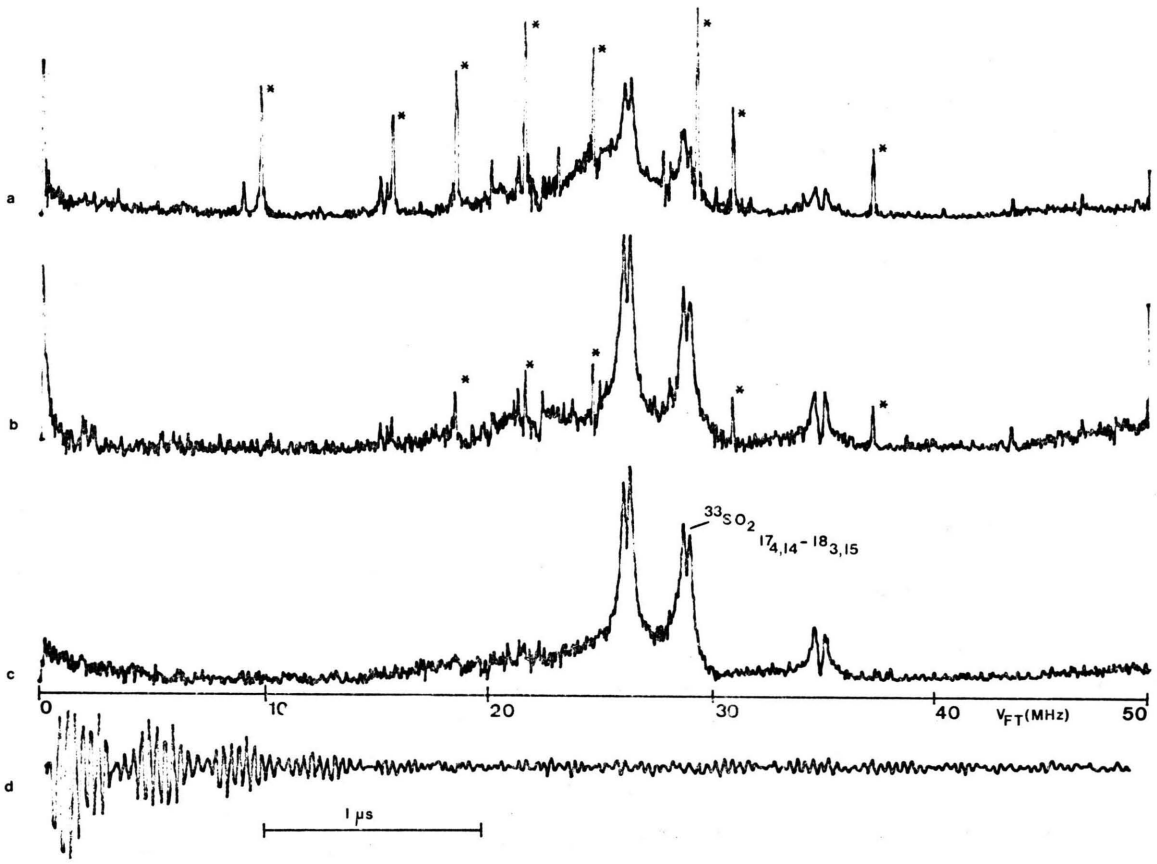

Fig. 9. 50 MHz scan out of the rotational spectrum of Sulphurdioxide, SO_2, $^{33}SO_2$ in natural abundance

$J_{K_-K_+} - J'_{K_-'K_+'} = 17_{4,14} - 18_{3,15}$; $\alpha_{\text{total}} = 6 \cdot 10^{-8}\,\text{cm}^{-1}$.

1024 data points incremented by 1024 zeros, MW-signal frequency 16 758.25 GHz, MW-pulse 100 ns, pressure $p = 5.7$ mTorr, temperature $T = 300\,°\text{K}$. a) 64 K cycles without baseline subtraction measuring time $t_m = 14$ s. b) 96 K cycles with baseline subtraction (48 K with, 48 K without MW-pulse), $t_m = 21$ s. c) subtraction of two measurements like b); second measurement with phase inverted IF, $t_m = 42$ s. d) transient decay curve for c.

* coherent disturbance.

angular frequency of the molecular transition with dipole matrix element μ_{ab} ($\varkappa = 2\,\mu_{ab}/\hbar$). ε_0 is the electric field amplitude of the microwave pulse at the beginning of the absorption cell and t_p is the pulse duration.

ΔN_0 is the population difference of the transition at equilibrium and c_g is the microwave group velocity. The transient emission signals are observed for times $t \geqq \tau_1$. A damping constant α_g has been introduced in (1) to account phenomenoligically for the cell attenuation which gives rise to a damping of both the exciting and emitted radiation.

No analytical solution of the integral in (1) has been found for general microwave pulses which are characterized by duration t_p and amplitude ε_0 and a numerical analysis of (1) has to be performed to obtain the dependence of E_{em} on cell length L in the general case.

To simplify the analysis we replace the Bessel function in (1) by a sine function, $J_1(\varkappa\,\varepsilon_0\,t_p\,e^{-\alpha_g z/2}) \cong \frac{1}{2}\sin(\varkappa\,\varepsilon_0\,t_p\,e^{-\alpha_g z/2})$, which gives a result holding for a plane wave:

$$E_{em} = F(t)\,e^{-\alpha_g L/2}\int_0^L \sin(\varkappa\,\varepsilon_0\,t_p\,e^{-\alpha_g z/2})\,e^{\alpha_g z/2}\,dz \qquad (2)$$

with

$$F(t) = -\frac{\pi\,\omega\,\hbar\,\varkappa\,\Delta N_0}{2\,c_g}\,e^{-(t-\tau_1)/T_2}.$$

Considering the dependence of signal amplitude on the cell length L in (2) we obtain maximum change

in signal if

$$dE_{em}/dL = 0 . \tag{3}$$

Carrying out the differentiation of (2) with respect to L gives

$$dE_{em}/dL = F(t) e^{-\alpha_g L/2} \{\sin(\varkappa \varepsilon_0 t_p) + \varkappa \varepsilon_0 t_p \{Ci(\varkappa \varepsilon_0 t_p e^{-\alpha_g L/2}) - Ci(\varkappa \varepsilon_0 t_p)\}\} \tag{4}$$

where Ci is the cosine integral function.

With (3) and (4) the optimum cell length L_{op} may be determined numerically for fixed values of α_g and $\varkappa \varepsilon_0 t_p$.

The dependence of signal amplitude on pulse duration t_p may also be investigated within the limit of approximation (2). A maximum in emission signal is obtained for a pulse duration satisfying the condition

$$dE_{em}/dt_p = 0 . \tag{5}$$

Differentiating (2) with respect to t_p gives

$$\frac{dE_{em}}{dt_p} = -2 F(t) e^{-\alpha_g L/2} \frac{\varkappa \varepsilon_0}{\alpha_g} \cdot \{Ci(\varkappa \varepsilon_0 t_p e^{-\alpha_g L/2}) - Ci(\varkappa \varepsilon_0 t_p)\} . \tag{6}$$

Combining the conditions (3) and (5) for optimum cell length L_{op} and optimum pulse duration $t_{p,op}$ gives with (4) and (6) the condition for $t_{p,op}$

$$\sin(\varkappa \varepsilon_0 t_{p,op}) = 0 \tag{7}$$

which defines a π-pulse at the beginning of the absorption cell

$$\varkappa \varepsilon_0 t_{p,op} = \pi . \tag{8}$$

Then, for a typical attenuation constant $\alpha_g = 1.15 \times 10^{-3}\,cm^{-1}$ or 0.5 dB/m an optimum cell length $L_{op} = 26.7$ m is obtained by means for Eqs. (3) and (4) if (8) is satisfied.

The emitted field amplitude which results with (2) and the values for L_{op} and $t_{p,op}$ ($E_{em} = 10.9 \times F(t)$ for $\alpha_g = 1.15 \times 10^{-3}\,cm^{-1}$) may be compared to the emission signal as obtained for shorter cell length. Thus for a 12 m absorption cell the optimum pulse duration is shorter ($\varkappa \varepsilon_0 t_p \cong 2.2$) and the field amplitude is about 80% of the optimum value.

A closed expression for L_{op} may be obtained for short pulses with the restriction

$$\varkappa \varepsilon_0 t_p \ll 1 \tag{9}$$

which is only applicable in favourable cases.

Then, by using the series expansion of the first order Bessel function

$$J_1(x) = \frac{1}{2} x - \frac{1}{16} x^3 + \cdots , \tag{10}$$

we may rewrite (1) considering only the first order term in (3)

$$E_{em} = -\frac{\pi \omega \hbar \varkappa^2 \varepsilon_0 \Delta N_0 t_p}{c_g} e^{-\alpha_g L/2} L e^{-(t-\tau_1)/T_2} = G(t) L e^{-\alpha_g L/2} . \tag{11}$$

Considering the dependence of signal amplitude E_{em} on the cell length L in (11) we obtain maximum change in signal if

$$dE_{em}/dL = G(t)\left(1 - \frac{\alpha_g}{2} L\right) e^{-\alpha_g L/2} = 0 . \tag{12}$$

With (12) the optimum cell length L_{op} is given by

$$L_{op} = 2/\alpha_g \tag{13}$$

a result which also holds for conventional microwave spectrometers [10]. Then, for $\alpha_g = 1.15 \times 10^{-3}\,cm^{-1}$ an optimum cell length of 17.4 m is obtained.

It is easy to show that (6) is also valid for the experimental arrangement of separated parts of the absorption cell (see discussion above) as long as the first order approximation (3) is well satisfied. Then, the additional loss due to the inserted ferrite isolators gives only rise to additional damping of the signal without changing the functional form of the L-dependence of the emitted field.

Sensitivity

We noticed that the limitation of our spectrometer sensitivity is presently not given by noise but by coherent disturbances, which we reduced by a large amount by different precautions in the construction given above. To reduce the coherent disturbances further a baseline substraction was incorporated in the 1-bit transient recorder/digital averager. In alternating sequence the transient signal produced by a polarizing MW-pulse and the transient disturbance without a pulse are measured and substracted. This diminishes the noise reduction by $\sqrt{2}$. The result is demonstrated in Figures 9 a, b.

Another method of suppressing the coherent disturbances is a phase shifting method as it is used in FT-NMR instruments [11]. If the MW of the

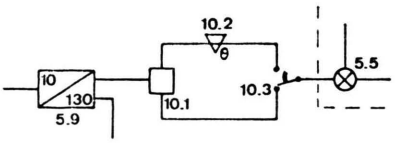

Fig. 10. Modification of the detection system (see Fig. 5) for alternating IF phase. 5.5 IF mixer; 5.9 Frequency multiplier; 10.1 180° power divider; 10.2 phase shifter for adjustment; 10.3 Manual coaxial switch.

polarizing pulse is shifted alternatively from 0 to 180° and back in consecutive pulses and the induced transient signals are added and subtracted respectively, coherent disturbances not correlated to this phase shift are suppressed without a sacrifice of the improvement of S/N ratio. The phase change of the MW pulse may be replaced by a phase change of the MW local or IF local frequency. In this case the suppression should be reduced however as coherent disturbances on the MW or IF local frequency respectively cannot be cancelled. As the phase changing is simplest for the IF frequency and independent from the used MW frequency we started preliminary experiments with this alternative. The set up of Fig. 5 was changed as given in Figure 10. Figure 9 c gives a result.

The two other alternatives are presently being tested. Figures 11 and 12 give the lines with the smallest absorption coefficient in the order of $10^{-9}\,\mathrm{cm}^{-1}$ we measured up to now. In this case the power of a transient emission is in the order of $5 \cdot 10^{-17}$ W. The measuring time was 960 and 300 s. It should noticed that a sharp line with a long transient decay is easier to measure than a broad line of the same height as the measuring time T is more effectively utilized for a sufficiently long decay.

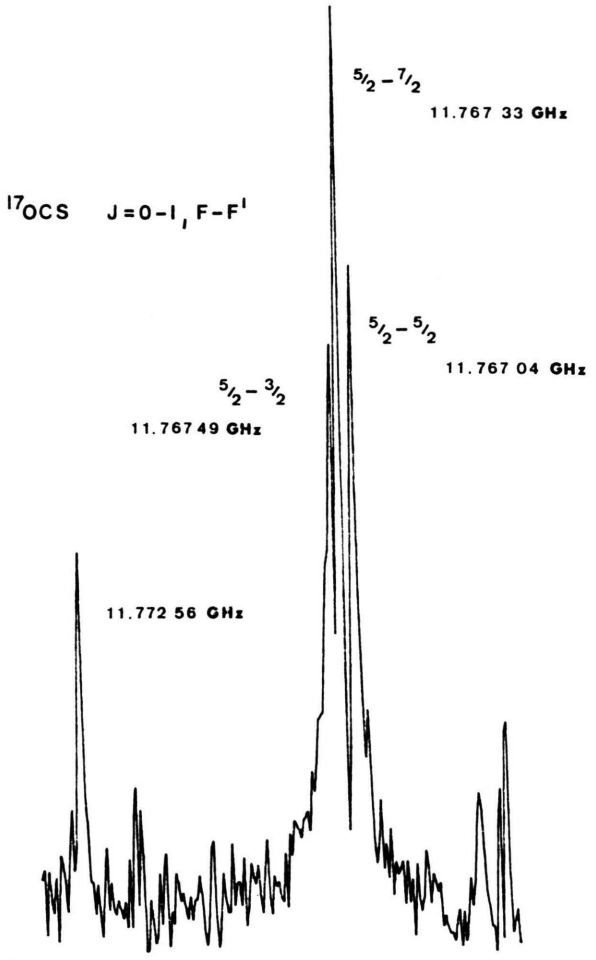

Fig. 11. A range of 10 MHz out of a 50 MHz scan of the OCS rotational spectrum. ^{17}OCS in natural abundance $J - J' = 0 - 1$, $\alpha_{\mathrm{total}} = 6 \cdot 10^{-9}\,\mathrm{cm}^{-1}$; $\alpha_{5/2-3/2} = 1.3 \cdot 10^{-9}\,\mathrm{cm}^{-1}$, measuring time 960 s for 50 MHz; MW signal frequency 11.764 GHz, $p = 5$ mTorr; $T = 213$ K, 1024 data points incremented by 1024 zeros.

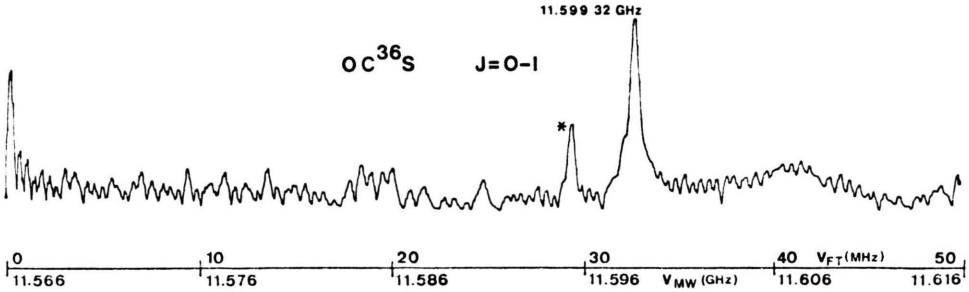

Fig. 12. 50 MHz scan of the OCS rotational spectrum, OC^{36}S in natural abundance, $J - J' = 0 - 1$, $\alpha = 3.4 \cdot 10^{-9}\,\mathrm{cm}^{-1}$ measuring time $t_m = 300$ s, MW signal frequency 11596.0 MHz, $p = 24$ mTorr, $T = 228$ K, 1024 data points.

* coherent disturbance.

Frequency Measurement and Resolution

The frequency of a spectral line is determined after the Fourier transformation from the set of Fourier coefficients $p_k = \sqrt{a_k^2 + b_k^2}$. The a_k are the cosine, the b_k are the sine transformation coefficients. They are related to the frequency by

$$\nu_k = k/N\,\Delta t \tag{14}$$

with $k = 0, \ldots, N/2$, N number of data points in the time domain, Δt digitizing step width. We determine the line maximum by a three point parabolic interpolation. We estimate that depending on the S/N ratio the frequency error is 0.1 to $0.2 \cdot 1/N \cdot \Delta t$ or 10 to 20 kHz for $N\,\Delta t = 1024 \cdot 10$ ns which is of the same order as in Stark spectroscopy. Other interpolation procedures will hardly improve the precision as an isolated line is determined only by few points (5 to 7 point). Increasing the number N of data points will be more effective.

A larger error results presently from the inaccuracy of the digitizing step width Δt. We believe, that a free running oscillator in the transient digitizer is not adequate. As we use a medium quality quartz in the transient digitizer, to control the step width, the error can be corrected. For this correction we have to measure the transient signal with the MW local oscillator 160 MHz above(+) and below (−) the signal frequency. After IF mixing with 130 MHz we get the line frequencies $\nu^{(+)}$ and $\nu^{(-)}$

$$\begin{aligned}
\nu^{(+)} &= \nu_{\mathrm{MW,signal}} - (30\,\mathrm{MHz} - \nu_{\mathrm{FT}}{}^{(+)}) \\
&\quad \text{for } \nu_{\mathrm{MW,local}} < \nu_{\mathrm{MW,signal}}\,, \\
\nu^{(-)} &= \nu_{\mathrm{MW,signal}} + (30\,\mathrm{MHz} - \nu_{\mathrm{FT}}{}^{(-)}) \\
&\quad \text{for } \nu_{\mathrm{MW,local}} > \nu_{\mathrm{MW,signal}}
\end{aligned} \tag{15}$$

with the IF frequency in the range $0 \leqq \nu_{\mathrm{FT}}{}^{(\pm)} \leqq 50$ MHz, calculated with (14) and $\Delta t = 10$ ns.

In the mean is

$$\begin{aligned}
\nu &= \frac{1}{2}\,(\nu^{(+)} + \nu^{(-)}) \;= \nu_{\mathrm{MW,signal}} \\
&\quad + \frac{1}{2}\,(\nu_{\mathrm{FT}}{}^{(+)} - \nu_{\mathrm{FT}}{}^{(-)})\,.
\end{aligned} \tag{16}$$

The errors compensate if $\nu_{\mathrm{FT}}{}^{(-)} - \nu_{\mathrm{FT}}{}^{(+)} \ll 50$ MHz which is fulfilled in the middle of the IF-frequency range. So we estimate the frequency precision to ± 20 KHz for $N = 1024$ and $\Delta t = 10$ ns, when the compensation is made. To overcome this disadvantage we plan to replace the 100 MHz quartz by a synchronized oscillator related to the frequency standard.

In Table 1 we give frequencies for comparison. As an accurate line shape analysis is difficult due to the low point number neighbouring lines are only resolved if the Fouriercoefficients fulfil the conditions *:

$$a_k > a_{k+1} \quad \text{and} \quad a_{k+2} > a_{k+1}\,. \tag{17}$$

* Here we refer to the cosine transformation.

Table 1. Comparison of calculated frequencies ν_{calc} (taken from Maki [12]) with measured frequencies by Stark- (ν_{St}) and FT- (ν_{FT})-spectroscopy. [a] Not resolved from $5/2 \rightarrow 7/2$ component. [b] Measured only with stabilisation of local oscillator 160 MHz higher than signal oscillator.

Molecule	Transition $J \rightarrow J'$	$F \rightarrow F'$	Vibrational State $v_1 v_2{}^l v_3$	Calculated ν_{calc} [MHz]	Measured Frequency ν_{St} [MHz]	ν_{FT} [MHz]
$^{16}O^{12}C^{32}S$	$0 \rightarrow 1$		0 0° 0	12162.99	12162.98	12162.98 (2)
$^{18}O^{12}C^{32}S$	$0 \rightarrow 1$		0 0° 0	11409.72	11409.71	11409.73 (2)
$^{16}O^{12}C^{34}S$	$0 \rightarrow 1$		0 0° 1	11830.30	11830.29	11830.32 (2)
$^{16}O^{13}C^{34}S$	$0 \rightarrow 1$		0 0° 0	11823.47	11823.46	11823.45 (2)
$^{16}O^{12}C^{36}S$	$0 \rightarrow 1$		0 0° 0	11599.36	11599.34	11599.32 (2)
$^{16}O^{12}C^{33}S$	$0 \rightarrow 1$	$3/2 \rightarrow 1/2$	0 0° 0	12004.02	12004.01	12004.03 (2)
		$3/2 \rightarrow 3/2$		12017.12	12017.10	12017.13 (2)
		$3/2 \rightarrow 5/2$		12011.30	12011.29	12011.31 (2)
$^{17}O^{12}C^{32}S$	$0 \rightarrow 1$	$5/2 \rightarrow 3/2$	0 0° 0	11767.53	[a]	11767.49 [b]
		$5/2 \rightarrow 5/2$		11767.14	11767.12	11767.04
		$5/2 \rightarrow 7/2$		11767.42	11767.41	11767.33

With (14) follows for the maximum resolution:

$$\Delta\nu = \nu_{k+2} - \nu_k = \frac{2}{N\,\Delta t} \tag{18}$$

which is 200 kHz with our present set up. Figure 11 demonstrates this fact. It may be improved increasing $N\,\Delta t = T$ [5].

Here we assume implicitely that the lines are narrow enough. For two lines of equal height and line maxima corresponding to the coefficients a_k and a_{k+2} (17) implies

$$T_2 > T/2\,\pi\,\sqrt{2} \tag{19}$$

assuming Lorentzian line profile.

For $T = 1024 \cdot 10$ ns this condition is usually fulfilled for low pressures ($\lesssim 10$ m Torr).

Conclusion

In this paper we report on our experiences with Fourier transform spectroscopy in the microwave region. Details of the construction of a Ku-band MW-FT-spectrometer are given and the feature of the apparatus are discussed. As demonstrated with the spectra of rotational transitions of OCS isotopes, the sensitivity of the FT-spectrometer is sufficient to record rotational lines with absorption coefficients as low as $\alpha \cong 10^{-9}\,\mathrm{cm}^{-1}$ with a reasonable S/N-ratio (>10). As compared to a conventional Stark-modulated microwave spectrometer the times which are necessary to record such weak spectra over a range of 50 MHz are considerably shorter with the Fourier transform method.

Due to the limited number of data points the accuracy of the line frequency determination is presently restricted to about 20 kHz. By the same reasons only lines which are separated more than 100 kHz may be resolved. However the inherent resolution of the FT method is in advantage to frequency domain spectroscopic methods which exhibit additional line broadening due to power saturation and modulation.

In addition to the measurement of microwave spectra of stable molecules in the ground electronic state, the FT spectroscopy may be useful for the investigation of rotational spectra in transient conditions as each measuring cycle takes only a few microseconds. Thus unstable species or rotational transitions in metastable excited vibronic states may be investigated. Further application of the spectrometer has proved to be useful for the determination of rotational relaxation times by measuring the transient response of the molecular sample shortly after the pulse excitation.

Appendix

Equation (1) may be obtained by considering the solutions of the wave equation for the emitted field and accounting phenomenologically for power loss due to wall attenuation. For a lossless rectangular waveguide and wave propagation in the TE_{10}-mode the contribution of polarized molecules in the layer between z and $z+\mathrm{d}z$ to the amplitude E_{em} of the emitted field at $z = L(x = a/2)$ is given by [13]

$$\mathrm{d}E_{\mathrm{em}} = -\frac{\pi\,\omega\,\hbar\,\varkappa\,\Delta N_0}{c_g} J_1(\varkappa\,\varepsilon_0\,t_p)\,e^{-(t-\tau_1)/T_2}\,\mathrm{d}z\,. \tag{A.1}$$

To derive (A.1) the frequency of the signal oscillator has assumed to be resonant with the molecular transition frequency which implies identical group velocities of the pulse and the emitted radiation *. In addition, to derive the initial condition for the polarization after pulse excitation ($\sim \sin(\varkappa\,\varepsilon_0\,t_p)$), relaxation phenomena have been neglected during the pulse period t_p ($t_p \ll T_2$).

To account for wall attenuation we have assumed an exponential damping of the microwave field in the sample which is described by a decay constant $\alpha_g/2$. Then the electric field amplitude ε_0 in (A.1) for a lossless waveguide has to be replaced by the z-dependent expression

$$\varepsilon = \varepsilon_0\,e^{-\alpha_g z/2} \tag{A.2}$$

where ε_0 specifies the electric field amplitude of the MW pulse at the beginning of the sample cell.

The attenuation of the emitted field due to wall losses has also to be considered. Thus the contribution $\mathrm{d}E_{\mathrm{em}}$ (A.1) to the emitted field at $z = L$ depends on the path difference $L - z$ which introduces a damping factor $e^{-\alpha_g(L-z)}$. Carrying out the corrections of (A.1) and integrating from 0 to L gives the final result for the total field at the end of the sample cell

$$E_{\mathrm{em}} = -\frac{\pi\,\omega\,\hbar\,\varkappa\,\Delta N_0}{c_g} e^{-\alpha_g L/2} \left\{\int_0^L J_1(\varkappa\,\varepsilon_0\; e^{-\alpha_g z/2}) \cdot e^{\alpha_g z/2}\,\mathrm{d}z\right\} \times e^{-(t-\tau_1)/T_2}\,. \tag{A.3}$$

* An extended treatment including off-resonance excitation has been given recently [13] and shows that (A.1) holds in good approximation for the more general case at the usual experimental conditions.

Acknowledgement

We thank the members of our group for many discussions and especially Dr. J. Wiese for drawing our attention to the phase alternating pulse technique and Prof. Dr. D. Sutter for critically reading the manuscript. Further we thank the workshop of our institute for the craftmanship and the Deutsche Forschungsgemeinschaft and the Fonds der Chemischen Industrie for funds.

[1] G. A. Vanasse and H. Sakai, Progress in Optics (E. Wolf ed.) **6**, 259 (1963), North Holland, Amsterdam.
[2] R. J. Bell, Introductory Fourier Transform Spectroscopy, Academic Press, New York 1972.
[3] T. C. Farrar and E. D. Becker, Pulse and Fourier NMR, Academic Press, New York 1971.
[4] J. C. McGurk, H. Mäder, R. T. Hofmann, T. G. Schmalz, and W. H. Flygare, J. Chem. Phys. **61**, 3759 (1974).
[5] J. Ekkers and W. H. Flygare, Rev. Sci. Instrum. **47**, 448 (1976).
[6] G. Bestmann, H. Dreizler, and H. Mäder, Z. Naturforsch. **34a**, 1330 (1979).
[7] W. Schrepp, G. Bestmann, and H. Dreizler, Z. Naturforsch. **34a**, 1467 (1979).
[8] J. C. McGurk, T. G. Schmalz, and W. H. Flygare, Advances in Chemical Physics (I. Prigogine and S. A. Rice ed.), Vol. XXV, p. 1, John Wiley, New York 1974.
[9] D. Ziessow, On-line Rechner in der Chemie, p. 66, Walter de Gruyter, Berlin 1973.
[10] C. H. Townes and A. L. Schawlow, Microwave Spectroscopy, p. 414, McGraw Hill Book Co, New York 1955.
[11] e.g. Bruker Physik AG, CXP-spectrometer.
[12] A. G. Maki, J. Phys. Chem. Ref. Data **3**, 221 (1974).
[13] T. G. Schmalz and W. H. Flygare, Laser and Coherence Spectroscopy (J. I. Steinfeld ed.), p. 125, Plenum Press, New York 1978.